

ORIGINAL RESEARCH ARTICLE

Simulation study of calcaneal insertion in the treatment of children's flat foot

Elsa Nápoles-Padrón¹, Juan Pablo Pacheco-González¹, Raide A. González-Carbonell^{1*}, Armando Ortiz-Prado², Jesús Hernández-de la Torre¹

^{*1} Universidad de Camagüey Ignacio Agramonte Loynaz, Facultad de Electromecánica, Camagüey 70100, Cuba.
E-mail: raide1977@gmail.com

² Universidad Nacional Autónoma de México, Facultad de Ingeniería, Ciudad de México 999085, Mexico

ABSTRACT

One of the correction methods of children's flat foot is calcaneal insertion. The purpose of this work is to determine the performance of calcaneal stop by using two bioco MPatible materials. The Finite Element Method (FEM) is used. The material analysis is AISI 316L steel and Ti-6Al-4V titanium alloy. Using Cuban anthropometric models, loads were calculated based on foot biomechanics and body weight of boys and girls aged 10 and 12. The results show that the implant model ensures the mechanical strength of the two materials. The difference between the two stresses is 4.44 MPa, accounting for 5% of the difference. Both materials have enough mechanical strength reserves because the maximum stress is less than the elastic limit of the material and ensures the mechanical strength of the calcaneal stop design.

Keywords: finite element method; calcaneal insertion point; flat foot; biomechanics

1. Introduction

The foot is an important part of the body because it ensures our flexibility and balance. One of the most common causes affecting the foot is known as flat feet. Some conservative alternatives, such as the use of orthopedic shoes, brackets and insoles, have been used for flat foot correction. And only in cases where the previous treatments do not work, surgical correction is indicated^[1,2].

One known technique is the so-called calcaneal stop, which includes placing a screw in the tarsal

sinus (bone) to maintain the formation of the plantar fornix^[1,3]. The purpose of using calcaneal insertion implant is to correct the flat foot immediately after surgery. Orthopedic surgeons have evaluated its results as a good treatment option with less complications and good surgical effect^[4,5].

There are various types of calcaneal insertion implants, also known as prostheses, screws or devices. The mechanical properties of the element made of the human body must meet the conditions of its exposure. Titanium and its alloys and some stainless steel are used for this implant. Research on new materials such as those that are absorbed by

ARTICLE INFO

Received: June 8, 2020 | Accepted: July 19, 2020 | Available online: August 4, 2020

CITATION

Nápoles-Padrón E, Pacheco-González JP, González-Carbonell RA, et al. Simulation study of calcaneal insertion in the treatment of children's flat foot. *Wearable Technology* 2020; 1(2): 14–19.

COPYRIGHT

Copyright © 2020 by author(s). This is an Open Access article distributed under the terms of the Creative Commons Attribution License (<https://creativecommons.org/licenses/by/4.0/>), permitting distribution and reproduction in any medium, provided the original work is cited.

the body are among the current trends^[6,7]. The mechanical strength of these orthopedic implants can be evaluated by biomechanical research and numerical methods, in order to further improve the design or material substitution decision-making.

Among these methods, finite element method (FEM) is an indispensable modeling tool in many engineering fields and other branches of science and technology. In the past decade, the use of FEM in health fields such as disease prognosis and glaucoma has increased^[8,9], in examining the stress and deformation of dental implants^[10], and fatigue analysis of spinal pedicle screws^[11]. Research on feet using FEM appears in specialized scientific literature, such as fractures and injuries in this part of the human body^[12,13], work related to gait level^[14] and diseases related to diabetic feet^[15,16]. For the benefit of preventive medicine, research prior to the use of new screws is convenient. Therefore, the purpose of this work is to evaluate the behavior of stress, deformation and displacement in calcaneal implant stopper using FEM for children's flat foot correction,

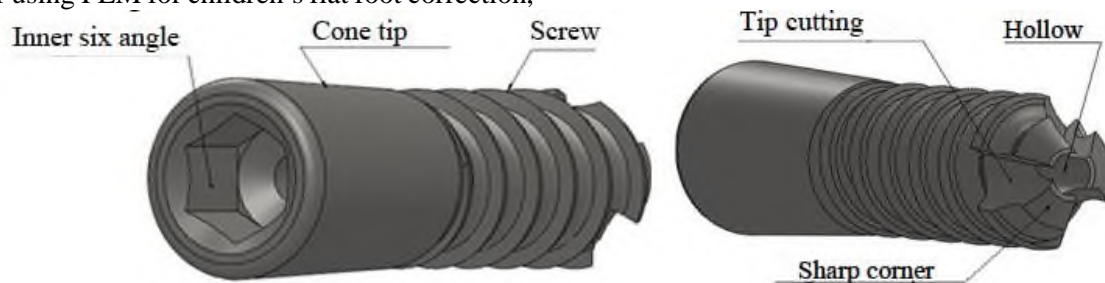


Figure 1. Geometric model of calcaneal insertion.

The head of the device is a smooth cone, which serves as a buffer for the heel and is used to correct the flat foot. The latter has a hexagon inside for screw implantation. Screws are the type used for cancellous bone to ensure the self-tightness of bone and prevent screw loosening. The tip has three 120° displacement cuts. This type of tip replaces the use of drill bit. Through a through-hole intubation at the longitudinal end, the screw can be placed correctly, and only a small incision needs to be made on the skin. Finally, the angle of the screw end ends at an angle of 90°, which helps to place the implant at the beginning of implantation.

so as to make decisions based on the evaluation of mechanical strength.

2. Methods and materials

The finite element method is used as a modeling method to study stress, strain and displacement. The implementation steps of FEM are composed of geometric model, load model, material model and grid model^[17]. Then it describes the process of obtaining components from the model.

2.1. Geometric model

Patent US 8267977 B2^[18] was selected as a result of the search for patents related to calcaneal implant stop to evaluate the characteristics, performance and technical specifications that best meet the needs of the study. According to the recommendations of orthopedic experts, this geometry makes the surgical process simpler and less invasive to bone and surrounding tissues, as shown in **Figure 1**.

2.2. Load model

The load on the implant depends on the child's weight. There is a relationship between boys' weight and age. According to the percentile data and chart of Cuban boys' weight from male and female age groups^[19], the maximum percentile weight of boys and girls aged 10 and 12 was selected to ensure the maximum load on the implant.

On the other hand, the plantar dome has three arches and supporting points. The load on the support point is uneven. In the upright, vertical and stationary position, 50% or 60% of the weight can

affect the calcaneus, while 50% or 40% of the weight can affect the anterolateral and anterolateral support. It is considered that in an upright, vertical and immobile position, 50% or 60% of the weight can be placed on the calcaneus, while in the antero-external and antero-internal supports 50% or 40%^[20,21]. **Figure 2** shows the support point of the foot and the load distributed according to the weight of the person. The authors believe that the force acting on the implant is 60% of the child's body weight. **Table 1** shows the weight, load and percentage information

corresponding to the calcaneus. The maximum load is 330.7 N, which is suitable for 12-year-old girls. It is the load used to analyze the strength and stiffness of implants.

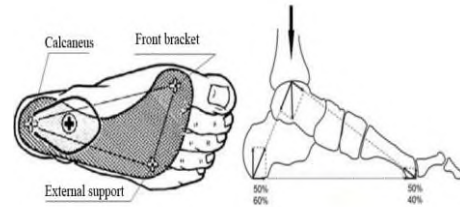


Figure 2. Foot support points and load distribution^[20,21].

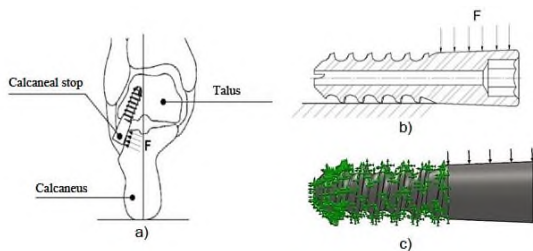
Table 1. Force ratio acting on the implant in each case

Age	Weight (kg)		Total load (n)		60%(N)	
	Masculine	Feminine	Masculine	Feminine	Masculine	Feminine
10	43.7	45.5	428.6	446.2	257.2	267.7
12	49.2	56.2	482.5	551.1	289.5	330.7

During the simulation, it should be considered that the screw is screwed on the calcaneus and the head is in contact with the calcaneus to form the plantar dome and correct the flat foot, **Figure 3a**. Therefore, the screw will be embedded in the screw area to simulate a consistent connection with the bone, while a distributed load is applied to the head, the value of which is discussed in the previous paragraph. **Figure 3b** shows the model loads and boundary conditions applied to the model.

Because of their mechanical strength, elastic limit, fatigue strength, wear resistance and fracture toughness, these two metal materials are widely used in the manufacture of orthopedic implants to replace or fix bones or joints. Both are bio-compatible and are accepted by living tissues.

According to ASTM standards, titanium alloy containing 6% aluminum and 4% vanadium is classified as grade 5, which is the most ductile alloy in grade 5. This is why it is one of the most recommended and commercialized implant manufacturing because of its high corrosion resistance and relatively low density than steel^[22]. In addition, compared with other biocompatible metal materials, AISI 316L stainless steel of surgical quality is suitable for the manufacture of implants because of its durability and low cost. Among other properties, it has been widely studied and has many international standards that specify its chemical composition, recommendations on which implant to use, and mechanical properties determined according to the method of acquisition, Annealing by plastic deformation^[23]. These materials are homogeneous and linearly isotropic, and their most common properties are shown in **Table 2**.



- (a) The insertion mode of the implant to realize that the plantar dome curls on the calcaneus and the head performs the cushioning function
- (b) The representation of the load condition, which applies the distributed load on the head and is embedded into the screw
- (c) The load model is represented in the simulation software, and the green arrow eliminates the movement

Figure 3. The load model of the calcaneal implant stops according to the position of the foot.

2.3. Material model

The materials used for modeling are titanium alloy (Ti-6Al-4V) and AISI 316L stainless steel.

Table 2. Mechanical properties of selected materials

Attribute	AISI 316L steel	Ti-6Al-4V Alloy
Modulus of elasticity (MPa)	200,000	110,000
Shear modulus (MPa)	82,000	41,023.81
Elastic limit (MPa)	200-500	795
Poisson coefficient	0.265	0.31
Maximum deformation (%)	55-60	10
Density (g/cm ³)	7.9	4.5

2.4. Grid model

Mesh generation is very important for element analysis and research. For this type of parts, the software recommends using solid mesh type (tetrahedron) and standard mesh (automatic three-dimensional). There are 9,934 elements and 16,479 nodes in total, as shown in **Figure 4**.

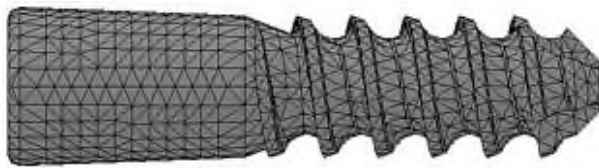
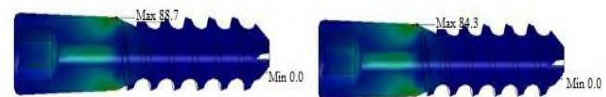


Figure 4. Insertion point of calcanal reticular implant.

3. Results and discussion

The study used two of the most commonly used surgical implant materials to study the mechanical strength of implants. The highest von Mises equivalent stresses have a value of 88.73 MPa for the implant made of AISI 316L steel (**Figure 5a**) and 84.29 MPa for those made of Titanium Ti-6Al-4V alloy (**Figure 5b**). The difference between the two stresses is 4.44 MPa, accounting for 5%. Therefore, according to the engineering standard, the difference is not significant. As shown in **Figure 5**, the maximum equivalent stress is located between the screw head and the screw transition zone. At this point, the diameter of the cone head is small and is the end of the depression. This result is consistent with the behavior of the cantilever beam, in which the stress increases towards the outer edge of the ge-

ometry, and the maximum value appears in the area near the bottom. This is a key part of this work.



(a) AISI 316L stainless steel is 88.73 MPa **(b)** titanium-ti-6al-4v alloy is 84.29 MPa

Figure 5. Calcanal implant insertion and other effects.

The elastic limit of titanium alloy can reach 795 MPa^[22], while the elastic limit of AISI 316L steel depends on its state (annealing or plastic deformation), ranging from 200 MPa to 500 MPa^[24]. Both materials have very good design factors because in all possible cases, the stress is less than the elastic limit of the material and ensures the mechanical strength of the calcanal stopper design.

The deformations have a maximum value of 3.741×10^{-4} for 316L steel (**Figure 6a**) and 7.024×10^{-4} for Ti-6Al-4V titanium alloy (**Figure 6b**). These deformations occur in the transition region between the screw head and the screw, which matches the distribution of equivalent stress. The deformation of alloy steel is about half that of titanium alloy.



(a) AISI 316L stainless steel 3.741×10^{-4} **(b)** titanium alloy Ti-6Al-4V 7.024×10^{-4}

Figure 6. The load deformation diagram of calcanal implant dead center.

This is because the elastic modulus of titanium

alloy is twice that of alloy steel, as shown in **Table 2**. Therefore, the unit deformation of titanium should be twice that of stainless steel. The equivalent stress difference between the implant and the two materials is less than 5%. Therefore, according to the law of elasticity, the proportional relationship between stress and strain is satisfied.

The maximum displacement of AISI 316L steel (**Figure 7a**) is 3,913 μm and that of Ti-6Al-4V titanium alloy (**Figure 7b**) is 7,394 μm . This displacement occurs at the end of the screw head, in the area of the maximum diameter of the cone. The results show that the stiffness of titanium alloy implant is low. These two displacements are insignificant compared with the displacement printed on the calcaneus by the implant. In order to form the plantar fornix, the calcaneus and calcaneus need to be separated by a few millimeters.



(a) AISI 316L stainless steel 3,913 μm , (b) Ti-6Al-4V titanium alloy 7,394 μm

Figure 7. Displacement diagram of insertion stop of calcaneus.

From the modeling results, AISI 316L stainless steel and titanium alloy can be used because they can resist the working conditions to which the implant will be exposed, because the elastic limit of both materials is much higher than the stress generated in the implant. It should be noted that AISI 316L stainless steel implants should be removed after the correction period, because the corrosion of these liquids will degrade the material after long-term exposure to body fluids^[25].

The position of the maximum equivalent stress close to the screw thread is consistent with the report in^[11], which analyzes the analysis of Ti-6Al-4V titanium alloy pedicle internal fixation. Different loading conditions are analyzed, and the fillet part of the thread is restrained concave.

The main limiting factor of the analyzed model is that it does not include the influence of fluctuating load during walking. However, AISI 316L has a minimum safety factor of 2.38, so it can be assumed

that the screw can resist fatigue conditions. The safety factor of titanium alloy Ti-6Al-4V is greater than 9. In addition, in further analysis, the screw bone interaction after the screw is inserted into the foot model should be considered, and the friction effect between bone and screw should be considered.

4. Conclusions

The implant model ensures the mechanical strength of the studied material. The maximum equivalent stress of AISI 316L steel implant is 88.73 MPa, and that of Ti-6Al-4V titanium alloy implant is 84.29 MPa. The percentage difference between the two tensions is 5%. Both materials have enough reserves in terms of mechanical strength, because they are far less than the elastic limit of the material and ensure the mechanical strength of the calcaneal stopper design.

Conflict of interest

The authors declare no conflict of interest.

References

1. Pavone V, Vescio A, Di Silvestri CA, et al. Outcomes of the calcaneo-stop procedure for the treatment of juvenile flatfoot in young athletes. *Journal of Pediatric Orthopedics* 2018; 12(6): 582–589.
2. Calvo S, Marti CR, Rasero PM, et al. Más de 10 años de seguimiento de la técnica de calcáneo stop [Calcaneal insertion technique was followed up for more than 10 years]. *Revista Española de Cirugía Ortopédica y Traumatología* 2016; 60(1): 75–80.
3. Pinho CF, Costa G, Santos CM, et al. Long-term outcomes of calcaneo-stop procedure in the treatment of flexible flatfoot in children: A retrospective study. *Acta Med Port* 2017; 20(7–8): 541–545.
4. Samaila E, Ggelmini M, Invernizzi E, et al. Low incidence of complications of arthroereisis with Calcaneo-Stop at long term follow-up. *Foot and Ankle Surgery* 2017; 23(Suppl.1): 71.
5. Fleites Lafont LM, Oscar Marrero Riverón CL, Alcalá Alfonso EJ. Técnica calcáneo-stop con elongación de tendones peroneos en el pie plano de pacientes con parálisis cerebral infantil [Calcaneal-stop technique with peroneal tendon elongation in flat feet in patients with infantile cerebral palsy]. *Revista Cubana de Ortopedia y Traumatología* 2014; 28(1): 39–57.
6. Giannini S, Cadossi M, Mazzotti A, et al. Bioab-

- sorbable calcaneo-stop implant for the treatment of flexible flatfoot: A retrospective cohort study at a minimum follow-up of 4 years. *Journal of Foot and Ankle Surgery* 2017; 56(4): 776–782.
7. Faldini C, Mazzotti A, Panchera A, et al. Patient-perceived outcomes after subtalar arthroereisis with bioabsorbable implants for flexible flatfoot in growing age: A 4-year follow-up study. *European Journal of orthopedic surgery and Traumatology* 2018; 8(4): 707–712.
 8. Calderín Pérez B, González Carbonell RA, Landín Sorí M, et al. Aplicabilidad de la simulación computacional en la biomecánica del disco óptico [Application of computational simulation in optic disc biomechanics]. *Arch Med Camagüey* 2015; 19(1): 73–82.
 9. Calderín Pérez B, González Carbonell RA, Landín Sorí M, et al. Análisis biomecánico del disco óptico bajo la variación de presión intraocular y rigidez escleral [Biomechanical analysis of optic disc under changes of intraocular pressure and scleral hardness]. *Rev. Cubana. Inv. Bioméd* 2016; 35(2): 136–157.
 10. Pérez Pozo L, Briones Picheira F, Aguilar Ramírez C. Análisis de esfuerzos mediante el método de elementos finitos de implantes dentales de titanio poroso [The stress of porous titanium implant was analyzed by finite element method]. *Ingeniería y Desarrollo* 2015; 33(1): 80–97.
 11. Cárdenas Oliveros JA, Cárdenas Caña JH, Teixeira Da Silva JM. Tornillo intrapedicular y prisionero. Análisis por el Método de Elementos Finitos [Intrapedicular and stud bolt. Analysis by the finite element method]. *Ingeniería Mecánica* 2017; 20(3): 129–135.
 12. Ouyang H, Deng Y, Xie P, et al. Biomechanical comparison of conventional and optimized locking plates for the fixation of intraarticular calcaneal fractures: A finite element analysis. *Comput Methods Biomech Biomed Engin* 2017; 20(12): 1339–1349.
 13. Wong D, Niu W, Wang Y, et al. Finite element analysis of foot and ankle impact injury: Risk evaluation of calcaneus and talus fracture. *PLoS ONE* 2016; 11(4): 1–14.
 14. Shih Cherng L, Carl Pai-Chu C, Simon Fuk-Tan T, et al. Stress distribution within the plantar aponeurosis during walking—A dynamic finite element analysis. *Journal of Mechanics in Medicine & Biology* 2014; 14(4): 1–17.
 15. Telfer S, Erdemir A, Woodburn J, et al. What has finite element analysis taught us about diabetic foot disease and its management? A systematic review. *PLoS ONE* 2014; 9(10): e109994.
 16. Guiotto A, Sawacha Z, Guarneri G, et al. 3D finite element model of diabetic neuropathy foot: A Gait analysis driven approach. *Journal of Biomechanics* 2014; 47(12): 3064–3071.
 17. González Carbonell RA, Álvarez García E, Campos Pérez Y. Tacón de torque. Análisis tensional y deformacional utilizando el Método de Elementos Finitos [Torque heel. Stress and deformation analysis using the Finite Element Method]. *Ingeniería Mecánica* 2007; 10(2): 79–83.
 18. Roth S (inventor). Titanium implants injected to correct children's flat feet. USA patent: US 8, 267,977 B2. 2012.
 19. Álvarez Sintés R. *Medicina General Integral [Comprehensive General Medicine]*. 3rd ed. Havana: Medical Science Press; 2014.
 20. Álvarez C, Palma VW. Desarrollo y biomecánica del arco plantar [Development and biomechanics of plantar arch]. *Ortho-tips* 2010; 6(4): 215–222.
 21. Viladot Voegeli A. Anatomía funcional y biomecánica del tobillo y el pie [Functional anatomy and biomechanics of ankle and foot]. *Rev Esp Reumatol* 2003; 30(9): 469–477.
 22. Elias CN, Lima JHC, Valiev R, et al. Biomedical applications of titanium and its alloys. *JOM* 2008; 60(3): 46–49.
 23. Disegi J [Internet]. Implant materials Wrapped with 18% chromium, 14% nickel and 2.5% molybdenum stainless steel. Synthes, West Chester, USA, 2009 [cited 2019 Jan 20]. Available from: <https://docplayer.net/22402352-Third-edition-implant-materials-wrought-18-chromium-14-nickel-2-5-molybdenum-stainless-steel.html>.
 24. Bartolomeu F, Buciumeanu M, Pinto E, et al. 316L stainless steel mechanical and tribological behavior—A comparison between selective laser melting, hot pressing and conventional casting. *Additive Manufacturing* 2017; 16: 81–89.
 25. Sierra Uribe JH, Bravo Molina, OM, et al. Evaluación electroquímica de recubrimientos de biovidrio/Al₂O₃ soportados sobre acero inoxidable AISI 316L y su relación con el carácter bioactivo de las películas [Electrochemical evaluation of bioglass/Al₂O₃ coating on AISI 316L stainless steel and its relationship with bioactivity of films]. *Revista Latinoamericana de Metalurgia y Materiales* 2015; 35(2): 151–164.